FEBS Letters 514 (2002) 78–83 FEBS 25794

Functional evidence for D- and T-loop interactions in tmRNA

Sharief Barends[a], Karl Björk[a], Alexander P. Gultyaev[b], Maarten H. de Smit[a], Cornelis W.A. Pleij[a], Barend Kraal[a,*]

[a] *Department of Biochemistry, Leiden Institute of Chemistry, Leiden University, P.O. Box 9502, 2300 RA Leiden, The Netherlands*
[b] *Group Theoretical Biology and Phylogenetics, Institute of Evolutionary and Ecological Sciences, Leiden University, Kaiserstraat 63, 2311 GP Leiden, The Netherlands*

Received 1 November 2001; accepted 5 November 2001

First published online 28 January 2002

Edited by Lev Kisselev

Abstract During bacterial protein synthesis, stalled ribosomes can be rescued by tmRNA, a molecule with both tRNA and mRNA features. The tRNA region of tmRNA has sequence similarity with $tRNA^{Ala}$ and also has a clover-leaf structure folded similarly as in canonical tRNAs. Here we propose the L-shape of tmRNA to be stabilized by two tertiary interactions between its D- and T-loop on the basis of phylogenetic and experimental evidence. Mutational analysis clearly demonstrates a tertiary interaction between G_{13} and U_{342}. Strikingly, this in evolution conserved interaction is not primarily important for tmRNA alanylation and for binding to elongation factor Tu, but especially for a proper functioning of SmpB.

Key words: tmRNA; Ala-tRNA synthetase; Elongation factor Tu; SmpB; tRNA folding; *trans*-Translation

1. Introduction

Escherichia coli tmRNA is a 363-nucleotide molecule with hybrid features of both tRNA and mRNA. This remarkable molecule was first found to rescue ribosomes stalled in their translation of truncated mRNAs and to tag the unfinished protein for degradation [1–3]. Moreover, it is now becoming clear that bacteria can use tmRNA as a key-role player in other translation-control mechanisms [4,5]. For further details of the elegant tmRNA *trans*-translation mechanism, see [6–9].

The tRNA-like part of the *E. coli* tmRNA is formed by a long-distance interaction between its 5′ and 3′ ends which show sequence homology with *E. coli* $tRNA^{Ala}$. This part folds into a near-perfect acceptor stem and T-hairpin, as supported by phylogenetic comparisons combined with chemical and enzymatic probing data [10–12]. A distinct anticodon-arm structure is not present in tmRNA. In the D-region, no obvious D-stem can be observed. Several lines of experimental evidence support the existence of a tRNA-like structure. (1) In analogy to the T-loop consensus sequence TΨCRANY of canonical tRNA, the *E. coli* tmRNA contains two modified nucleotides in its T-loop structure: T_{341} and Ψ_{342} [13]. (2) Precursor *E. coli* tmRNA interacts with processing enzymes for canonical tRNAs, such as RNase P, RNase III, RNase E and ATP/CTP tRNA nucleotidyl transferase [14–17,8]. (3) Mature tmRNA interacts with alanyl-tRNA synthetase (AlaRS) and becomes alanylated [14]. Subsequently, alanyl-tmRNA forms a ternary complex with elongation factor Tu and GTP (EF-Tu·GTP) [18,19]. Compared to $tRNA^{Ala}$, the interactions of tmRNA with AlaRS and EF-Tu·GTP appear to be significantly less stable [18]. For the proper functioning of tmRNA, an additional protein SmpB is indispensable [6]. As we recently found, SmpB has a high affinity for both tmRNA and $tRNA^{Ala}$, and interacts with the acceptor arm-like structure of tmRNA [45]. There, it stimulates the alanylation of tmRNA. In contrast, binding of SmpB to $tRNA^{Ala}$ results in inhibition of its alanylation.

A physical study, by means of transient electric birefringence and modelling of the three-dimensional structure of tmRNA, showed that the angle between its helix 2 and acceptor arm is significantly larger (110–140°) than that between anticodon- and acceptor arms of canonical tRNAs [20]. A chemical study by means of UV-induced intramolecular cross-linking showed the proximity of U_9/U_{10} in the D-region with C_{346}/U_{347} in the T-loop [21]. In the proposed model, the D- and T-loops have parallel tertiary interactions between the conserved $G_{13}G_{14}$ in the D-region and $\Psi_{342}C_{343}$ in the T-loop, with further stabilization by the T_{341}–A_{345} tertiary interaction in the T-loop. These interactions are identical to those stabilizing the overall structure of canonical tRNAs. For tmRNA, these interactions have been proposed by several groups but have so far not been supported by functional experiments [13,20–22]. In the present paper, we provide such evidence by mutational and functional analysis.

2. Materials and methods

2.1. Construction of tmRNA and $tRNA^{Ala}$ mutants

The mutations in *E. coli* tmRNA were introduced by PCR with the following primer pairs from Gibco BRL (*Eco*RI and *Bam*HI sites are underlined, the T7 promoter region is in italics and mutations are in bold): tmRNA (wt 5′) 5′-GATTAC<u>GAATTC</u>*TAATACGACTCACTATAG*GGGCTGATTCTGGATTCGACGGG-3′, tmRNA (wt 3′) 5′-GAGA<u>GGATCC</u>TGGTGGAGCTGGAGAGAGTTGAACCCGCGTAAG-3′; tmRNA (G_{13}A 5′) 5′-GATTAC<u>GAATTC</u>*TAATACGACTCACTATAG*GGGCTGATTCTAGATTCGACGGG-3′, tmRNA (U_{342}G 3′) 5′-GAGA<u>GGATCC</u>TGGTGGAGCTGGAGAGAGTTGCACCCGCGTAAG-3′.

PCR products were purified on gel (Qiagen) and digested with *Eco*RI/*Bam*HI prior to ligation (Promega protocol) into the *Eco*RI/*Bam*HI-linearized and gel-purified plasmid pT710Sa#21 [8]. Ligation mixtures were precipitated in 70% (v/v) ethanol in the presence of 5 μg/μl bulk tRNA (Sigma). Plasmids were introduced into competent JM109 cells by electroporation and were afterwards checked for cor-

*Corresponding author. Fax: (31)-71-5274340.
E-mail address: b.kraal@chem.leidenuniv.nl (B. Kraal).

0014-5793/02/$22.00
PII: S0014-5793(02)02306-2

rect sequences by means of a T7 sequencing kit (Amersham-Pharmacia).

For the mutations in *E. coli* $tRNA^{Ala}$, a different approach was followed. The following 5′-phosphorylated primers were designed with *Eco*RI and *Bam*HI overhangs (font styles as above): $tRNA^{Ala}$ (wt coding 5′) 5′-AATTCCTGCAG*TAATACGACTCACTATAG*GGGCTATAGCTCAGCTG-3′, $tRNA^{Ala}$ (wt non-coding 5′) 5′-GCGCTCTCCCAGCTGAGCTATAGCCCCTATAGTGAGTCGTATTACTGCAGG-3′, $tRNA^{Ala}$ (wt coding 3′) 5′-GGAGAGGCGTTGCTATGCAAGCAAGAGGTCAGCGGTTCGATCCCGCTTAGCTCCACCAG-3′, $tRNA^{Ala}$ (wt non-coding 3′) 5′-GATCCTGGTGGAGCTAAGCGGGATCGAACCGCTGACCTCTTGCTTGCATAGCAA-3′, $tRNA^{Ala}$ ($G_{18}A$ coding 5′) 5′-AATTCCTGCAG*TAATACGACTCACTATAG*GGGCTATAGCTCAGCT**A**-3′, $tRNA^{Ala}$ ($G_{18}A$ non-coding 5′) 5′-GCGCTCTCC**T**AGCTGAGCTATAGCCCCTATAGTGAGTCGTATTACTGCAGG-3′, $tRNA^{Ala}$ ($U_{55}G$ coding 3′) 5′-GAGAGGCGTTGCTATGCAAGCAAGAGGTCAGCGGT**G**CGATCCCGCTTAGCTCCACCAG-3′), $tRNA^{Ala}$ ($U_{55}G$ non-coding 3′) 5′-GATCCTGGTGGAGCTAAGCGGGATCG**C**ACCGCTGACCTCTTGCTTGCATAGCAA-3′).

First, two complementary primers were mixed (10 μM each, in 20 μl water), incubated at 65°C for 10 min, and cooled down slowly to room temperature. Next, hybridized primer pairs constituting both 5′ and 3′ ends of the $tRNA^{Ala}$ were mixed (5 μM of each hybridized primer pair) and ligated in one step within the *Eco*RI/*Bam*HI-linearized and gel-purified pALA119 plasmid [23]. JM109 cells were transformed with ligation mixtures as described for tmRNA and the plasmids were checked by sequencing.

2.2. RNA and protein isolation; analysis of aminoacylation kinetics

All RNA species were obtained by in vitro run-off transcription on *Mva*I-linearized plasmid DNA with the T7 RiboMAX large-scale RNA-production system (Promega). For ^{32}P-labelling of RNAs, [α-^{32}P]UTP (3000 Ci/mmol) was used (Amersham-Pharmacia). Purification of RNAs, C-terminally $(His)_6$-tagged EF-Tu, AlaRS and SmpB (all from *E. coli*), and analysis of alanylation kinetics were performed as in [18,45].

2.3. Sequence alignments

From tmRNA databases ([25,26] and corresponding web sites), the sequences from 18 different lineages were aligned for their tRNA region by the Vector NTI 5 program with manual improvement. The tmRNAs are from the α-proteobacteria *Bradyrhizobium japonicum (Bj)*, *Caulobacter crescentus (Cc)*, *Rickettsia prowazekii (Rp)*, *Sinorhizobium meliloti (Sm)*, the β-proteobacteria *Bordetella pertussis (Bp)*, *Neisseria gonorrhoeae (Ng)*, the γ-proteobacteria *E. coli (Ec)*, *Pseudomonas aeruginosa (Pa)*, *Yersinia pestis (Yp)*, the δ-proteobacteria *Desulfovibrio vulgaris (Dv)*, *Geobacter sulfurreducens (Gs)*, the ε-proteobacteria *Campylobacter jejuni (Cj)*, *Helicobacter pylori (Hp)*, the firmicutes *Bacillus subtilis (Bs)*, *Mycoplasma genitalium (Mg)*, the cyanobacterium *Prochlorococcus marinus (Pm)*, the cyanelle (plastid) of the alga *Cyanophora paradoxa (Cp)* and the mitochondrion of the protist *Reclinomonas americana (Ra)*.

3. Results

3.1. Sequence comparisons of tmRNA structures

Since recently, all members of the eubacterial kingdom are known to contain a gene for tmRNA, or a split form of a permuted tmRNA gene such as for the α-proteobacteria and possibly for the mitochondria of the protist *R. americana* [27].

We aligned the tRNA-like regions of 18 different tmRNAs representing all subdivisions of the proteobacteria and organelles, and compared them with *E. coli* $tRNA^{Ala}$ in order to find consensus sequences for the equivalent D- and T-loop structures (Fig. 1). The alignments for α-proteobacterial and mitochondrial tmRNAs were fitted manually, because of their permuted nature [27]. Although the D-loop sequences show a great variability, there is a strict conservation at the positions corresponding to the invariant G_{19} (in D-loop) and C_{56} (in T-loop) of canonical tRNAs which have a parallel Watson–

			acc. stem	D-stem	D-loop	D-stem		T-stem	T-loop	T-stem	acc. stem	
α	*Bj* *	(120)	GGGGGCG		A-AAU**AG**-GAUCGA		… (53)	CCGGG	G**GC**GGUA	CCCGG	CGCCUCC	ACCA
	Cc *	(114)	GGGGCCG		A--UC**AG**-CAUCGA		… (56)	CCGGG	U**GC**GAUU	CCCGG	CGGCUCC	ACCA
	Rp *	(302)	GGGGGCG		A-AAU**AG**-GAUCGA		… (50)	UCGGG	G**GC**AGUA	CCCGA	CGCCUCC	ACCA
	Sm *	(113)	GGGGGCG		A-AAU**AG**-GAUCGA		… (54)	CCGGG	G**GC**GGUA	CCCGG	CGCCUCC	ACCA
β	*Bp*	(1)	GGGGCCG		AUCC-**GG**-AUUCGA		… (360)	GGGGG	U**UC**AAUU	CCCCC	CGGCUCC	ACCA
	Ng	(1)	GGGGGCG		ACCUU**GG**-UUUCGA		… (336)	GGGGG	U**UC**GAUU	CCCCC	CGCCUCC	ACCA
γ	*Ec*	(1)	GGGGCUG		AUUCU**GG**-AUUCGA		… (336)	GCGGG	U**UC**AACU	CCCGC	CAGCUCC	ACCA
	Pa	(1)	GGGGCCG		AUUA-**GG**-AUUCGA		… (326)	GGGGG	U**UC**AAAU	CCCCC	CGGUUCC	ACCA
	Yp	(1)	GGGGCUG		AUUCU**GG**-AUUCGA		… (337)	GGGGG	U**UC**AAAU	CCCCC	CAGCUCC	ACCA
δ	*Dv*	(1)	GGGGGCG		-CACU**GG**-UUUCGA		… (325)	GCGGG	U**UC**GAUU	CCCGC	CGCCUCC	ACCA
	Gs	(1)	GGGGGUG		-UACA**GG**-UUUCGA		… (329)	GCGGG	U**UC**GACU	CCCGC	CACCUCC	ACCA
ε	*Cj*	(1)	GGGAGCG		ACU-U**GG**-CUUCGA		… (332)	AGGGG	U**UC**GAUU	CCCCU	CGCUUCC	ACCA
	Hp	(1)	GGGGCUG		ACU-U**GG**AUUUCGA		… (359)	UGGGG	U**UC**GAUU	CCCCA	CAGCUCC	ACCA
firmic.	*Bs*	(1)	GGGGACG		-UUAC**GG**-AUUCGA		… (337)	GUGGG	U**UC**GACU	CCCAC	CGUCUCC	ACCA
	Mg	(1)	GGGGAUG		-UUUU**GG**-GUUUGA		… (365)	ACGGG	U**UC**GAUU	CCCGU	CAUCUCC	ACCA
cyanob.	*Pm*	(64)	GGGGUUG		U-AAU**GG**-UUUCGA		… (267)	GUGGG	U**UC**AAAU	CCCAC	CAGCUCC	ACCA
cyanelle	*Cp*	(1)	GGGGCUG		UUUA-**GG**-UUUCGA		… (30)	AGCGG	U**UC**GAUU	CCGCU	CAACUCC	A
mitoch.	*Ra* *	(123)	GGGGAUG		UUUUU**AG**UAUUCGA		… (74)	CCGAG	G**GC**GGAU	CUCGG	CAUCUCC	A
$tRNA^{Ala}$	*Ec*	(1)	GGGGCUA	GCUC	AG-CU**GG**-----GA	GAGC	… (49)	AGCGG	U**UC**GAUC	CCGCU	UAGCUCC	ACCA
consensus			**GGGY•YR**		**•••••GG•••••GA**			**•••RG**	**•UCRR••**	**CY•••**	**YR•YUCC**	**ACCA**

Fig. 1. Comparative tmRNA sequence analysis for different members of the α, β, γ, δ, ε proteobacteria, firmicutes, cyanobacteria and organelles, together with the canonical *E. coli* $tRNA^{Ala}$. For species abbreviations see Section 2.3. Nucleotides essential for the putative D-/T-loop interaction are in bold and linked by arrows. For the α-proteobacteria *Bj, Cc, Rp, Sm*, and for *Pm* and *Ra*, the nucleotide numbering appears inverted due to the permuted nature of these tmRNAs, and corresponds to the precursor RNAs. Asterisks indicate species with tmRNAs having the covariation A–G instead of the G–U pair.

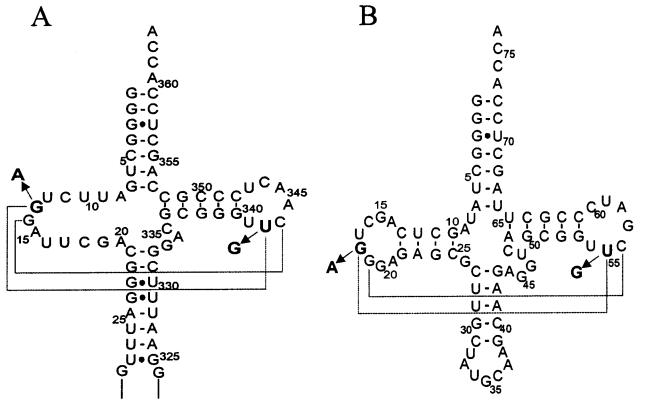

Fig. 2. Secondary structure of (A) the tRNA region of tmRNA and (B) $tRNA^{Ala}$. Helix 2 of tmRNA starts at a similar position as the anticodon stem of $tRNA^{Ala}$. Phylogenetic comparison (Fig. 1) suggests that G_{13}–U_{342} and G_{14}–C_{343} in tmRNA are at analogous positions as G_{18}–U_{55} and G_{19}–C_{56} in $tRNA^{Ala}$; the nucleotides involved in these (putative) tertiary interactions between D- and T-loops are connected with lines. The nucleotides analyzed in this study are printed in bold.

Crick pairing. A parallel non-Watson–Crick neighbour pair in tRNA is formed by the invariant G_{18} and Ψ_{55} (see Fig. 1, *E. coli* $tRNA^{Ala}$). In the different tmRNAs, analogous pairs of highly conserved residues occur, such as $G_{13}G_{14}$ and $U_{342}C_{343}$ for *E. coli* tmRNA (Fig. 1, in bold). In analogy to tRNA, tmRNA U_{342} is modified post-transcriptionally into Ψ_{342} [13]. In some cases, however, the G–U pair of the putative tertiary interaction is replaced by an A and G in the D- and T-loop, respectively (Fig. 1, see asterisk at α-proteobacterial and mitochondrial *Ra* tmRNA). This strict covariation indicates, that either the G–U or the A–G pair are involved in a tertiary interaction, and that this interaction is functionally important.

3.2. Alanylation kinetics of mutated tmRNA and $tRNA^{Ala}$ species

To support the putative tertiary interaction in *E. coli* tmRNA experimentally, we constructed mutant tmRNAs by replacing G_{13} in the D-loop with an A ($G_{13}A$), by replacing U_{342} in the T-loop with a G ($U_{342}G$), or by replacing both together ($G_{13}A$, $U_{342}G$). The double mutant tmRNA thus has the same covariation as occurs in α-proteobacteria and the protist mitochondrion. The homologous mutations were also introduced in *E. coli* $tRNA^{Ala}$ as a reference (see Fig. 2).

Table 1
Kinetic parameters for Ala–RNA complex formation with EF-Tu·GTP[a]

	k_{-1} ($\times 10^{-3}$ s^{-1})	k_1 ($\times 10^3$ M^{-1} s^{-1})	K_d ($\times 10^{-6}$ M)
tmRNA			
wt	4 ± 1.2	0.5 ± 0.1	8.0 ± 0.8
$G_{13}A$	2.4 ± 0.5	1.8 ± 0.5	1.3 ± 0.3
$U_{342}G$	5.0 ± 0.9	1.7 ± 0.4	2.9 ± 0.2
double	3.2 ± 0.2	0.3 ± 0.1	10.7 ± 0.5
$tRNA^{Ala}$			
wt	12 ± 2	77 ± 16	0.16 ± 0.01
$G_{18}A$	2.2 ± 0.7	3.5 ± 0.7	0.6 ± 0.2
$U_{55}G$	1.1 ± 0.1	0.7 ± 0.3	1.6 ± 0.1
double	7.2 ± 1.2	25 ± 8	0.29 ± 0.05

[a]Kinetic parameters were determined by the RNase A protection assay as described in [18,24]. The values result from three independent experiments.

For the determination of parameters of alanylation kinetics, initial rates of Ala–RNA formation were measured after 60 s of incubation for each tmRNA species, and after 20 s for each $tRNA^{Ala}$ species (except for $U_{55}G$ where alanylation was stopped after 60 s). The k_{cat}/K_M values in the Michaelis–Menten plots of Fig. 3 show that, relative to wild-type (wt) tmRNA, the $G_{13}A$ and $U_{342}G$ mutants have a 2.5- and 1.5-fold higher alanylation efficiency, respectively, mainly due to an increased k_{cat}. The k_{cat}/K_M for the double mutant is about 70% of the wt value. In marked contrast to tmRNA, the analogous mutations in $tRNA^{Ala}$, $G_{18}A$ and $U_{55}G$, cause a drop of two and three orders of magnitude in k_{cat}/K_M values, respectively, when compared to wt tmRNA. The double mutation restores the alanylation efficiency up to 10% of wt $tRNA^{Ala}$.

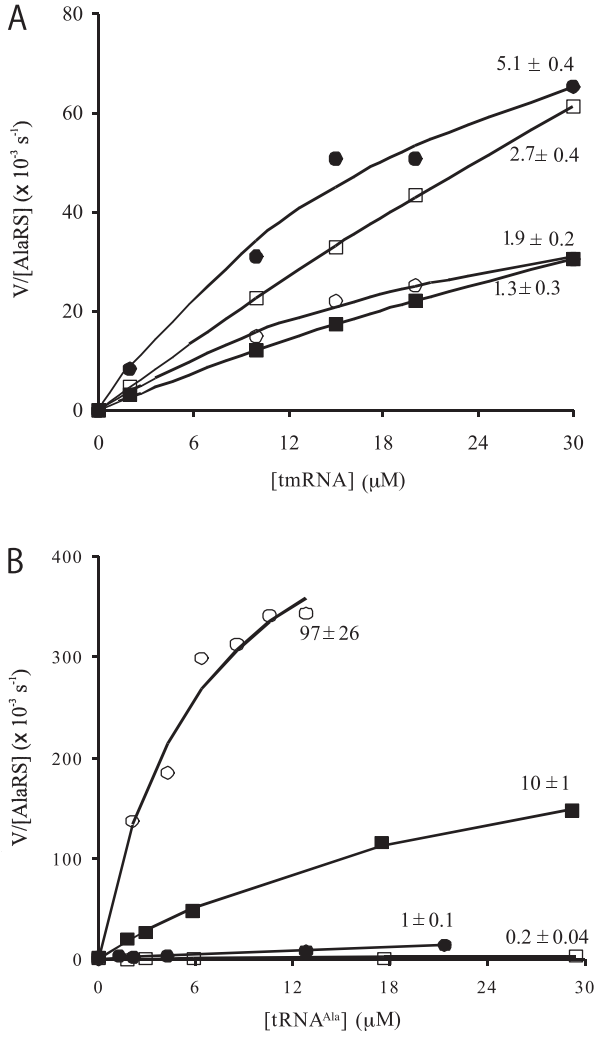

Fig. 3. Michaelis–Menten kinetics of alanylation by AlaRS. Initial rates were measured at different concentrations of tmRNA wt (○), $G_{13}A$ (●), $U_{342}G$ (□) and ($G_{13}A$, $U_{342}G$) (■) in (A) and of $tRNA^{Ala}$ wt (○), $G_{18}A$ (●), $U_{55}G$ (□) and ($G_{18}A$, $U_{55}G$) (■) in (B). The AlaRS concentration was 1 μM in the experiments with the tmRNAs and $tRNA^{Ala}$ $U_{55}G$, and 0.25 μM with the other $tRNA^{Ala}$ variants. The calculated k_{cat}/K_M values (10^3 $M^{-1}s^{-1}$) are next to the corresponding curves.

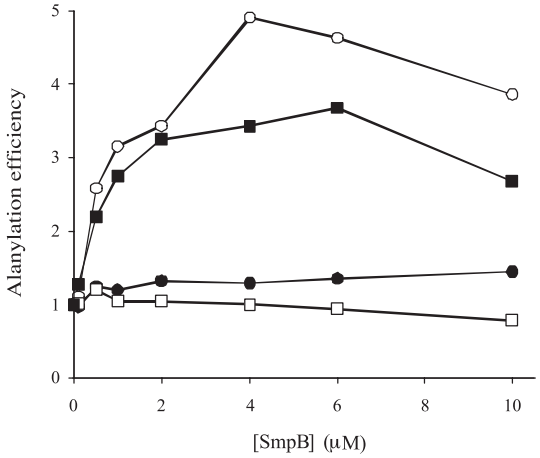

Fig. 4. SmpB effects on the alanylation of mutant tmRNAs. Initial rates were determined in the presence of 1 μM AlaRS with 1 μM tmRNA wt (○), $G_{13}A$ (●), $U_{342}G$ (□) or ($G_{13}A$, $U_{342}G$) (■) and are plotted as relative values (1.0 for wt).

3.3. EF-Tu affinity for mutant Ala-tmRNA and Ala-tRNA^{Ala} species

The effects of the mutations in tmRNA and tRNA^{Ala} on complex formation with EF-Tu·GTP were assessed by RNase A protection assays at 4°C with increasing concentrations of EF-Tu·GTP. From such experiments, constants for the dissociation rate (k_{-1}), the association rate (k_1) and the dissociation constant (K_d) can be calculated [24] and the results are listed in Table 1. Disruption of the proposed tertiary interaction within tmRNA, either by the mutation $G_{13}A$ or $U_{342}G$, causes 6- and 3-fold lower K_d values, respectively, mainly by a higher association rate k_1. The double mutant again shows comparable parameters for EF-Tu complex formation as wt tmRNA. For tRNA^{Ala}, destabilization of the D-/T-loop interaction has a less pronounced effect on EF-Tu complex formation than on alanylation. However, in contrast to the tmRNA mutants, the $G_{18}A$ and the $U_{55}G$ mutants exhibit a 4- and 10-fold higher K_d for EF-Tu–GTP, respectively, mainly due to a lower k_1. The double mutant has an affinity of 50% compared to wt tRNA^{Ala}.

3.4. A link between tertiary interactions in tmRNA and SmpB functioning

A third protein partner of mature tmRNA on its way to stalled ribosomes is SmpB [6]. SmpB has a high affinity for both tmRNA and tRNA^{Ala}, but only stimulates alanylation of tmRNA. We recently located the site of SmpB binding in the tRNA region of tmRNA [45]. Here, we have monitored the effect of increasing concentrations of SmpB on the alanylation of the mutant tmRNAs. Surprisingly, the stimulatory effect of SmpB on the alanylation of wt tmRNA is completely absent for the $G_{13}A$ and $U_{342}G$ mutants, but is restored for the double mutant (Fig. 4). This means that the single mutants may either have lost their affinity for SmpB, or that SmpB still binds but fails to stimulate alanylation.

To assess this, SmpB binding to the different tmRNAs was analyzed by band-shift experiments (Fig. 5). Increasing concentrations of SmpB led to comparable retardation of all the tmRNAs and the calculated K_d values of the complexes are all around 50 nM. Apparently, the failure of SmpB to stimulate the alanylation of the two single-mutant tmRNAs, $G_{13}A$ and $U_{342}G$, is not due to a reduced affinity, but rather to a loss of activation of their acceptor arm regions.

4. Discussion

The well-established secondary structure of the *E. coli* tmRNA shows a tRNA-like structure comprising both extremities of the molecule [10–19]. Several studies on its tertiary folding suggest a similar D-/T-loop interaction as in canonical tRNAs [13,20–22]. The present study investigates this model by phylogenetic sequence alignments and mutational analysis.

From the alignments it appears, that the tmRNAs have an almost invariant doublet combination of GG in the D-loop with UC (modified as ΨC) in the T-loop, the combination of AG with GC being the only exception. It looks as if an A–G

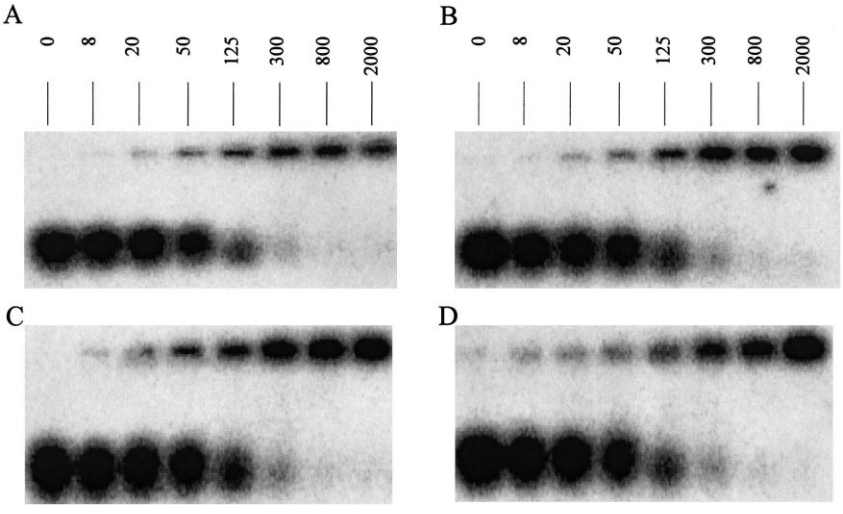

Fig. 5. Band-shift analysis of 1 nM (mutant-)tmRNA-complex formation at increasing concentrations (0–2000 nM) of SmpB. Electrophoresis was on 1% (w/v) agarose gel and quantification was by phosphor imaging. For tmRNA wt (A), $G_{13}A$ (B), $U_{342}G$ (C) and $G_{13}A$, $U_{342}G$ (D), the calculated K_d values are all around 50 nM.

pairing, suggested here for some tmRNAs, can also serve as a (partial) substitute for the G_{18}–Ψ_{55} pair in D-/T-loop interactions of other tRNA(-like) structures. This covariation was found in certain mitochondrial tRNAs [28,29]. Functionally active tRNA variants with this covariation have also been isolated by various in vitro selection procedures [30,31]. Interestingly, in staphylococcal $tRNA^{Gly}$ a substitution of Ψ by G in the T-loop is accompanied by a very unusual D-loop without an obvious base-pairing partner [32]; this special tRNA does not participate in protein synthesis but is active in peptidoglycan synthesis. Sequence comparisons and modelling of tRNA mimicry at the 3′ ends of tymo- and furoviruses of plants [33–35] also suggest an A–G pairing in their T-/D-loop interactions at the homologous location. In these plant viruses, the alternative covariation G–U (or G–Ψ) is less frequently found. Finally, we have found that a Turnip Yellow Mosaic Virus RNA double mutant with its original A–G pair at this position replaced by G–U is infectious, whereas the corresponding single mutants are less viable (de Smit et al., in preparation).

Thus, the comparison of tRNA-like structures from bacterial tmRNAs and plant viral RNAs suggests the presence of two parallel pairs of structurally homologous tertiary contacts between D- and T-loops, one of them being the invariant G–C pair equivalent to G_{19}–C_{56} in tRNA, and the other pair being either G–U (G–Ψ) or A–G and equivalent to G_{18}–Ψ_{55} in tRNA. The strict choice between these two alternatives indicates that the unusual covariation reflects isosteric pairing [36–38]. In tRNA molecules, the G_{18}–Ψ_{55} pair is known to have bifurcated pairing and consequently, the substitution of its Ψ/U by G is not followed by a second mutation into a 'mirror' U–G pair, because the bifurcated pairs are not self-isosteric [37].

The RNAs of our mutation studies were obtained by in vitro transcription and therefore do not contain any base modification. We have shown before that the in vitro synthesized tmRNA and $tRNA^{Ala}$ both maintain their biological activity in alanylation and EF-Tu complex formation [18]. Moreover, our results from highly specific lead-cleavage probing (not illustrated) indicate, that the non-modified $tRNA^{Ala}$ in vitro transcript still has the D-/T-loop interaction, in accordance to what was found for a $tRNA^{Phe}$ in vitro transcript [39]. This implies that base modifications are not essential for this tertiary interaction.

The two single mutations in tmRNA ($G_{13}A$ and $U_{342}G$) have a different effect on alanylation than the two corresponding mutations in $tRNA^{Ala}$, $G_{18}A$ and $U_{55}G$. Alanylation of the two tmRNA mutants appears to be more efficient than that of wt tmRNA, whereas alanylation of the two $tRNA^{Ala}$ mutants is virtually abolished. Both for tmRNA and $tRNA^{Ala}$, the double mutations restore alanylation to substantial levels. Similar effects of the mutations are visible for complex formation with EF-Tu, though much less pronounced.

The importance of the tertiary interactions between the D- and T-loops of canonical tRNAs for aminoacylation and EF-Tu complex formation has been demonstrated in various studies by others [30,31,40–43]. In vitro selection experiments revealed, that for these activities an A_{18}–G_{55} instead of the G_{18}–U_{55} is also functional in *E. coli* tRNAs for Leu and Phe [30,31]. This fits our results with $tRNA^{Ala}$, where the double mutant with A_{18}–G_{55} is a good substrate for alanylation and binding to EF-Tu. Another important feature of the D- and T-loop interaction emerges from mutational studies on $tRNA_2^{Gly}$. Using a negative in vivo selection procedure, mutant $tRNA_2^{Gly}$ species were isolated that were disturbed in ribosomal bypass efficiency during translation of the T4 gene *60* mRNA, but were still functional in normal translation [44]. The majority of the mutations were mapped at positions involved in tertiary interactions between the D- and T-loops, amongst others $G_{18}A$. Rigidity of the elbow structure thus appears to be critical for (possibly also EF-Tu controlled) codon–anticodon interaction during ribosomal bypassing. Altogether, the high degree of conservation of the tRNA nucleotides involved in D- and T-loop interaction is imposed by its cognate synthetase, to some extent by EF-Tu, and by a proper positioning on the ribosome.

Our results for tmRNA show interesting novel features and a more complicated situation. Destabilization of the putative D-/T-loop interaction makes tmRNA an even better substrate for both AlaRS and EF-Tu–GTP. To the best of our knowledge, no precedents exist for such effects due to destabilization of tRNA folding. Possibly, tmRNA does not fully mimic the folding of regular tRNA because 6 of the 9 stabilizing tertiary interactions in tRNA are not provided by the D-region of tmRNA [21]. Indeed, the angle at the elbow corner of the tmRNA acceptor arm is significantly larger (110–140°) than for canonical tRNA [20]. Since there is no anticodon recognition for tmRNA, a rigid D-/T-loop interaction is perhaps not required for a proper A-site positioning of Ala-tmRNA. Another essential factor for proper functioning of tmRNA on ribosomes is SmpB [6]. By binding to the tmRNA acceptor arm, it stimulates alanylation significantly [45]. Strikingly, SmpB only stimulates the alanylation of the wt and the double mutant tmRNA, but not that of both single mutants, $G_{13}A$ and $U_{342}G$. The absence of an SmpB effect on the latter two is not due to a lack of SmpB binding; the affinity is the same as for wt. Apparently, SmpB still binds, but is no longer able to further activate the tmRNA acceptor arm with a disrupted tertiary interaction. Next to stimulation of tmRNA alanylation, SmpB might facilitate a proper arrangement of Ala-tmRNA in the ribosomal A-site for which a correct tmRNA folding would be equally important.

Altogether, these results demonstrate the existence of a tertiary interaction between the D- and T-loop of tmRNA. Single mutations $G_{13}A$ or $U_{342}G$ in the conserved putative G_{13}–U_{342} pairing cause a substantial change in tmRNA functioning with its three different partners AlaRS, EF-Tu and SmpB, whereas the double mutation ($G_{13}A$, $U_{342}G$) (also found as a natural covariation) restores the original functioning. This is remarkable since tmRNA does not display the clear D-stem structure of canonical tRNA; the D-region is reduced to 10–13 nucleotides that cannot form the usual 3–4 bp. In various tmRNA models, a small D-stem structure is proposed (up to 2 bp usually). However, its location is not phylogenetically conserved, and moreover, the nucleotides involved are not conserved and do not display covariation.

The strong conservation of the G_{13}–U_{342} or A_{13}–G_{342} pairing in tmRNA is apparently not established by selective pressure for alanylation nor for EF-Tu–GTP binding; the single mutants actively interact. However, for proper functioning of SmpB, the D-/T-loop interaction is essential. This is a new evolutionary selection pressure on the high conservation of the D-/T-loop interaction, which is unique for tmRNA.

Acknowledgements: We thank Drs. A.W. Karzai and R.T. Sauer for their kind gift of SmpB, Drs. Ribas de Pouplana and Schimmel for the AlaRS expression plasmid, and Dr. J. Horowitz for pALA119. This work was supported by a Grant to S.B. and B.K. from the Council for Chemical Sciences of the Netherlands Organization for Scientific Research (CW-NWO, 328-035).

References

[1] Keiler, K.C., Waller, P.R. and Sauer, R.T. (1996) Science 271, 990–993.
[2] Muto, A., Ushida, C. and Himeno, H. (1998) Trends Biochem. Sci. 23, 25–29.
[3] Karzai, A.W., Roche, E.D. and Sauer, R.T. (2000) Nat. Struct. Biol. 7, 449–455.
[4] Abo, T., Inada, T., Ogawa, K. and Aiba, H. (2000) EMBO J. 19, 3762–3769.
[5] Roche, E.D. and Sauer, R.T. (2001) J. Biol. Chem. 23, 23.
[6] Karzai, A.W., Susskind, M.M. and Sauer, R.T. (1999) EMBO J. 18, 3793–3799.
[7] Williams, K.P., Martindale, K.A. and Bartel, D.P. (1999) EMBO J. 18, 5423–5433.
[8] Wower, I.K., Zwieb, C.W., Guven, S.A. and Wower, J. (2000) EMBO J. 19, 6612–6621.
[9] Lee, S., Ishii, M., Tadaki, T., Muto, A. and Himeno, H. (2001) RNA 7, 999–1012.
[10] Williams, K.P. and Bartel, D.P. (1996) RNA 2, 1306–1310.
[11] Felden, B., Himeno, H., Muto, A., McCutcheon, J.P., Atkins, J.F. and Gesteland, R.F. (1997) RNA 3, 89–103.
[12] Hickerson, R.P., Watkins-Sims, C.D., Burrows, C.J., Atkins, J.F., Gesteland, R.F. and Felden, B. (1998) J. Mol. Biol. 279, 577–587.
[13] Felden, B., Hanawa, K., Atkins, J.F., Himeno, H., Muto, A., Gesteland, R.F., McCloskey, J.A. and Crain, P.F. (1998) EMBO J. 17, 3188–3196.
[14] Komine, Y., Kitabatake, M., Yokogawa, T., Nishikawa, K. and Inokuchi, H. (1994) Proc. Natl. Acad. Sci. USA 91, 9223–9227.
[15] Li, Z., Pandit, S. and Deutscher, M.P. (1998) Proc. Natl. Acad. Sci. USA 95, 2856–2861.
[16] Lin-Chao, S., Wei, C.L. and Lin, Y.T. (1999) Proc. Natl. Acad. Sci. USA 96, 12406–12411.
[17] Srivastava, R.K., Miczak, A. and Apirion, D. (1990) Biochimie 72, 791–802.
[18] Barends, S., Wower, J. and Kraal, B. (2000) Biochemistry 39, 2652–2658.
[19] Rudinger-Thirion, J., Giegé, R. and Felden, B. (1999) RNA 5, 989–992.
[20] Stagg, S.M., Frazer-Abel, A.A., Hagerman, P.J. and Harvey, S.C. (2001) J. Mol. Biol. 309, 727–735.
[21] Zwieb, C., Guven, S.A., Wower, I.K. and Wower, J. (2001) Biochemistry 40, 9587–9595.
[22] Ushida, C., Himeno, H., Watanabe, T. and Muto, A. (1994) Nucleic Acids Res. 22, 3392–3396.
[23] Liu, J.C., Liu, M. and Horowitz, J. (1998) RNA 4, 639–646.
[24] Vorstenbosch, E.L., Potapov, A.P., de Graaf, J.M. and Kraal, B. (2000) J. Biochem. Biophys. Methods 42, 1–14.
[25] Williams, K.P. (2000) Nucleic Acids Res. 28, 168.
[26] Zwieb, C. and Wower, J. (2000) Nucleic Acids Res. 28, 169–170.
[27] Keiler, K.C., Shapiro, L. and Williams, K.P. (2000) Proc. Natl. Acad. Sci. USA 97, 7778–7783.
[28] Heckman, J.E., Hecker, L.I., Schwartzbach, S.D., Barnett, W.E., Baumstark, B. and RajBhandary, U.L. (1978) Cell 13, 83–95.
[29] Helm, M., Brule, H., Friede, D., Giegé, R., Putz, D. and Florentz, C. (2000) RNA 6, 1356–1379.
[30] Peterson, E.T., Blank, J., Sprinzl, M. and Uhlenbeck, O.C. (1993) EMBO J. 12, 2959–2967.
[31] Asahara, H., Nameki, N. and Hasegawa, T. (1998) J. Mol. Biol. 283, 605–618.
[32] Roberts, R.J., Lovinger, G.G., Tamura, T. and Strominger, J.L. (1974) J. Biol. Chem. 249, 4781–4786.
[33] Dumas, P., Moras, D., Florentz, C., Giegé, R., Verlaan, P., Van Belkum, A. and Pleij, C.W. (1987) J. Biomol. Struct. Dyn. 4, 707–728.
[34] Dreher, T.W. and Goodwin, J.B. (1998) Nucleic Acids Res. 26, 4356–4364.
[35] Goodwin, J.B. and Dreher, T.W. (1998) Virology 246, 170–178.
[36] Gautheret, D. and Gutell, R.R. (1997) Nucleic Acids Res. 25, 1559–1564.
[37] Leontis, N.B. and Westhof, E. (1998) Q. Rev. Biophys. 31, 399–455.
[38] Masquida, B. and Westhof, E. (2000) RNA 6, 9–15.
[39] Behlen, L.S., Sampson, J.R., DiRenzo, A.B. and Uhlenbeck, O.C. (1990) Biochemistry 29, 2515–2523.
[40] Puglisi, J.D., Putz, J., Florentz, C. and Giegé, R. (1993) Nucleic Acids Res. 21, 41–49.
[41] Sampson, J.R., DiRenzo, A.B., Behlen, L.S. and Uhlenbeck, O.C. (1990) Biochemistry 29, 2523–2532.
[42] Nazarenko, I.A., Harrington, K.M. and Uhlenbeck, O.C. (1994) EMBO J. 13, 2464–2471.
[43] Hou, Y.M. and Schimmel, P. (1992) Biochemistry 31, 4157–4160.
[44] Herr, A.J., Atkins, J.F. and Gesteland, R.F. (1999) EMBO J. 18, 2886–2896.
[45] Barends, S., Karzai, A.W., Sauer, R.T., Wower, J. and Kraal, B. (2001) J. Mol. Biol. 314, 9–21.